Electronic Supplementary Material (ESI) for RSC Advances

Supporting Information:
Electron impact on N_2/CH_4 mixtures in He droplets – Probing chemistry in Titan's atmosphere by S. Ptasinska et al.

Experimental Section

The experimental measurements were carried out at the University of Innsbruck by means of a commercial Time-of-Flight mass spectrometer (Tofwerk, H-TOF) coupled with a Nier-type ion source and a homebuilt helium (He) droplet source.[1] The droplet source consists of a shielded closed-cycle cryostat and a mechanically decoupled nozzle block. The Helium is pressurized to 2 MPa and cooled down to temperatures below 10 K along the cryostats cooling stages. The nozzle block connects to the second cooling stage with copper braids and a line for the Helium. The temperature of the nozzle block is controlled by a silicone diode and resistive counter heating. Its position can be adjusted during operation with a stage. Helium is expanded from the tip of the nozzle block through a 5 µm orifice into the vacuum chamber. The supersonic expansion forms an ultra-cold (0.37K) neutral beam of He-droplets with a narrow velocity and broad size distribution. After formation, the beam is skimmed and enters a differentially pumped pick-up chamber with 20 cm long region. Here the unique ability of He-droplets to pick up foreign species with high efficiency is then utilized to form clusters of N_2 and/or CH_4 molecules.

Gasses are introduced into the pick-up chamber through a regulated leak valve at a constant partial pressure of $4x10^{-3}$ Pa. For pick-up of both species, a mixture with the desired proportion is prepared in advance in a separate container. Since both molecules are heliophilic, they move to the centre of the droplet where they aggregate if multiple dopants are picked up. The

probabilities for subsequent pick-up follow a Poissonian distribution. During pick-up, evaporative cooling via loss of He atoms quickly removes excess energy from the system and keeps the temperature of the droplet at 0.37 K.

The doped droplets then enter a differentially pumped ion source chamber. In the ion source, the neutral droplet beam is crossed with a 70 eV electron beam. The electrons can form ions in different ways. Direct electron ionization of the dopant is very unlikely due to the dense Helium layers surrounding it. Penning ionization via He^* is also considered to have a negligible contribution to the presented measurements. The dopants are located inside the droplet while the heliophobic He^* stays on or close to the surface.[2] The main contribution is formation of He^+ and subsequent charge transfer to the dopant via resonant charge hopping.[3] This ionization process is introducing several eV of excess energy into the system which can – dependant on the dopant – result in fragmentation. Evaporative cooling can lessen the excess energy but not quench fragmentation entirely. The ionic cluster size distribution consequently differs from the neutral one.

The ions are accelerated towards the TOF-MS and guided into the extraction region with a stack of einzel lenses. The mass spectrometer uses a reflectron to enhance the effective mass resolution so that identification of isobaric ions in the low mass region is possible. For experiments with He-droplets this is especially important since many ion signals on nominal masses have several possible compositions such as CO^+ (27.994 Th), N_2^+ (28.006 Th) and He_7^+ (28.018 Th). The ions are finally detected with a multi-channel plate (chevron configuration) in single-ion counting mode.

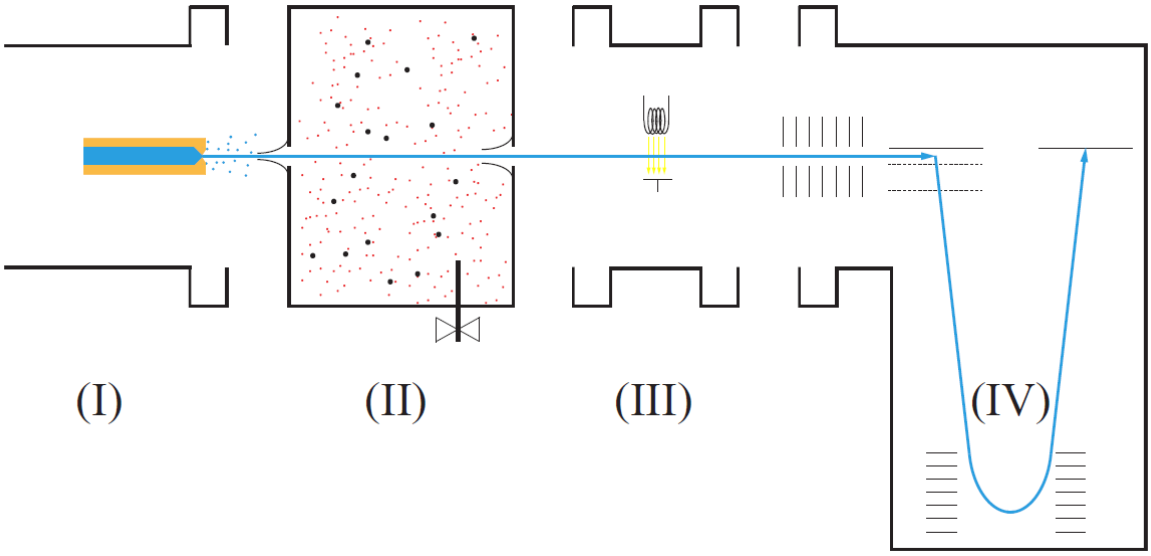

Fig. Schematic of the experimental apparatus. The helium nanodroplets are generated by supersoinc expansion in the cluster source region (I) and pass through a 10 cm to 20 cm long pick-up region (II) before they enter the ionization chamber (III). In this chamber the nanodroplets interact with an electron beam and cations are formed. The resulting cations are then mass analyzed by a time-of-flight mass spectrometer (IV).

Computational Methods

Geometry optimizations and vibrational frequencies were calculated at the CCSD level[4] with the 6-311G(2d,p) basis set,[5] followed by final single point electronic energy calculations at the CCSD(T) level[6] with the cc-pVTZ basis set[7] and were carried out with the QChem program.[8] The binding energies for all dimers include corrections for changes in zero-point vibrational energy (from CCSD/6-311G(2d,p)) and for basis set superposition error (from CCSD(T)/cc-pVTZ).

Cartesian coordinates for the species analyzed

N_2

1	N	0.000000	0.000000	-0.548440
2	N	0.000000	0.000000	0.548440

CH_3^+

1	C	0.000000	0.000000	0.000000
2	H	0.000000	0.000000	1.092181
3	H	-0.945856	0.000000	-0.546090
4	H	0.945856	0.000000	-0.546090

CH_4^+

1	C	-0.111016	-0.000022	0.000033
2	H	0.941628	0.000250	-0.550006
3	H	0.941938	-0.000221	0.549832
4	H	-0.608725	0.963777	0.000122
5	H	-0.608745	-0.963675	-0.000147

CH_5^+

1	C	0.122815	-0.010346	0.000000
2	H	0.263407	1.087076	0.000000
3	H	0.486353	-0.428066	-0.938070
4	H	0.486353	-0.428066	0.938070
5	H	-1.017498	0.382209	0.000000
6	H	-0.955507	-0.551079	0.000000

N_4^+

1	N	0.000000	0.000000	1.001460
2	N	0.000000	0.000000	2.102805
3	N	0.000000	0.000000	-1.001460
4	N	0.000000	0.000000	-2.102805

$CH_3N_2^+$(I)

1	C	0.000000	1.198266	0.000000
2	H	1.050327	1.489873	0.000000

3	H	-0.525164	1.489873	-0.909610
4	H	-0.525164	1.489873	0.909610
5	N	0.000000	-0.285639	0.000000
6	N	0.000000	-1.379962	0.000000

$CH_3N_2^+$(II)

1	C	0.000000	0.000000	2.339371
2	H	0.000000	0.000000	1.243341
3	H	0.942250	0.000000	2.891147
4	H	-0.942250	0.000000	2.891147
5	N	0.000000	0.000000	-0.956417
6	N	0.000000	0.000000	-2.052420

$CH_4N_2^+$(I)

1	C	-1.960316	-0.000306	0.000000
2	H	-0.537026	-0.001464	0.000000
3	H	-2.107806	1.082172	0.000000
4	H	-2.112827	-0.540586	-0.937113
5	H	-2.112827	-0.540586	0.937113
6	N	0.779474	0.001559	0.000000
7	N	1.882295	-0.001231	0.000000

$CH_4N_2^+$(II)

1	C	1.949359	0.002783	0.001608
2	H	2.100413	0.894327	0.608480
3	H	2.096416	0.083456	-1.074530
4	H	2.094759	-0.970142	0.469169
5	H	0.471163	-0.009697	-0.004824
6	N	-0.771465	-0.009988	-0.005164
7	N	-1.865522	0.007896	0.004029

$CH_5N_2^+$

1	C	-2.091704	0.048649	0.000010
2	H	-2.632608	-0.100866	-0.932841
3	H	-1.633190	1.053289	-0.000047
4	H	-2.632493	-0.100737	0.932955
5	H	-0.880721	-0.175047	-0.000119
6	H	-1.453756	-0.945334	0.000130
7	N	1.009544	-0.041881	-0.000080
8	N	2.102313	0.038567	0.000060

$CH_4CH_4^+$(I)

1	C	-1.683588	-0.007032	0.002631
2	C	1.683274	0.007470	-0.003166
3	H	-1.804148	-0.974282	0.483610
4	H	1.795272	1.001437	-0.428444
5	H	-1.926761	0.035261	-1.059233
6	H	-1.939217	0.864750	0.606104
7	H	1.936955	-0.826332	-0.658562
8	H	1.937525	-0.094703	1.052239
9	H	-0.447371	0.188642	-0.076039
10	H	0.449629	-0.197401	0.083535

$CH_4CH_4^+$(II)

1	C	1.516722	-0.013487	0.000000
2	H	0.168320	0.212601	0.000000
3	H	1.787718	0.482280	0.930924
4	H	1.787718	0.482280	-0.930924
5	H	1.487308	-1.102773	0.000000
6	C	-1.430897	-0.041870	0.000000
7	H	-2.300968	0.634926	0.000000
8	H	-1.373781	-0.621886	-0.917969
9	H	-1.373781	-0.621886	0.917969
10	H	-0.697485	0.866602	0.000000

REFERENCES

(1) Schöbel, H.; Leidlmair, C.; Bartl, P.; Aleem, A.; Hager, M.; Echt, O.; Märk, T.D.; Scheier, P. Ion–molecule reactions of ammonia clusters with C_{60} aggregates embedded in helium droplets. *Phys. Chem. Chem. Phys.* **2011**, *13*, 1092-1098.

(2) An der Lan, L.; Bartl, P.; Leidlmair, C.; Schöbel, H.; Jochum, R.; Denifl, S; Märk, T.D.; Ellis, A.M.; Scheier, P. The submersion of sodium clusters in helium nanodroplets: Identification of the surface - interior transition. *J. Chem. Phys.* **2011**, *135*, 044309-1 - 044309-6.

(3) Ellis, A. M.; Yang, S. Model for the charge-transfer probability in helium nanodroplets following electron-impact ionization. *Phys. Rev. A* **2007**, *76*, 032714-1 – 032714-8.

(4) Dalgaard, E.; Monkhorst, H. J. Some aspects of the time-dependent coupled-cluster approach to dynamic response functions. *Phys. Rev. A* **1983**, *28*, 1217-1222.

(5) Hehre, W. J.; Radom, L.; Schleyer, P. v. R.; Pople, J. A. *Ab Initio Molecular Orbital Theory*. Wiley: New York,
1986.

(6) Stanton, J. F.; Bartlett, R. J. The equation of motion coupled-cluster method. A systematic biorthogonal approach to molecular excitation energies, transition probabilities, and excited state properties. J. *Chem. Phys.* **1993**, *98*, 7029-7039.

(7) Dunning, Jr., T. H. *J. Chem. Phys.* **1989**, *90*, 1007-1023

(8) Shao, Y.; Fusti-Molnar, L.; Jung, Y.; Kussmann, J.; Ochsenfeld, C.; Brown, S. T.; Gilbert, A. T. B.; Slipchenko, L. V.; Levchenko, S. V.; O'Neill, D. P.; Distasio Jr., R. A.; Lochan, R. C.; Wang, T.; Beran, G. J. O.; Besley, N. A.; Herbert, J. M.; Lin, C. Y.; Van Voorhis, T.; Chien, S. H.; Sodt, A.; Steele, R. P.; Rassolov, V. A.; Maslen, P. E.; Korambath, P. P.; Adamson, R. D.; Austin, B.; Baker, J.; Byrd, E. F. C.; Dachsel, H.; Doerksen, R. J.; Dreuw, A.; Dunietz, B. D.; Dutoi, A. D.; Furlani, T. R.; Gwaltney, S. R.; Heyden, A.; Hirata, S.; Hsu, C.-P.; Kedziora, G.; Khalliulin, R. Z.; Klunzinger, P.; Lee, A. M.; Lee, M. S.; Liang, W.; Lotan, I.; Nair, N.; Peters, B.; Proynov, E. I.; Pieniazek, P. A.; Rhee, Y. M.; Ritchie, J.; Rosta, E.; Sherrill, C. D.; Simmonett, A. C.; Subotnik, J. E.; Woodcock III, H. L.; Zhang, W.; Bell, A. T.; Chakraborty, A. K.; Chipman, D. M.; Keil, F. J.; Warshel, A.; Hehre, W. J.; Schaefer III, H. F.; Kong, J.; Krylov, A. I.; Gill, P. M. W.; Head-Gordon, M. Advances in methods and algorithms in a modern quantum chemistry program package. *Phys. Chem. Chem. Phys.* **2006,** *8*, 3172-3191.